P3.4 **A SKIRTED RANKINE COMBINED VORTEX MODEL**

Vincent T. Wood[1] and Luther W. White[2]
[1]NOAA/OAR/National Severe Storms Laboratory,
[2]Department of Mathematics, University of Oklahoma, Norman, OK

1. INTRODUCTION

Tangential winds in such atmospheric vortices as dust devils, tornadoes, mesocyclones, waterspouts, landspouts, and tropical cyclones, to a first approximation, may be modeled as a classic Rankine (1882) combined vortex (henceforth RCV). The RCV consists of a core in solid-body rotation surrounded by a potential vortex where the tangential wind (V) is inversely proportional to radial distance (r) from the center of the vortex. The RCV model produces a top-hat profile of vertical vorticity in the vortex embedded in an irrotational environment (potential vortex). Furthermore, the model shows that circulation (defined as the basic measure of macroscopic rotation in a fluid, given by $\Gamma = 2\pi Vr$) varies as r^2 inside the RCV core and remains conserved outside the core in the potential flow (Davies-Jones and Wood 2006). This prediction is very crude owing to (a) the simplicity of the RCV model, and (b) the model's inherent discontinuity in vorticity and circulation at the vortex's core radius (R_x) where a peak tangential wind (V_x) occurs. This discontinuity cannot be a natural entity for viscous vortex flow.

To eliminate the discontinuity from the RCV model, we have developed an analytical "skirted" RCV (henceforth SRCV) model in which the radial profiles of tangential wind, vertical vorticity and circulation create (a) a smooth transition between the inner and outer profiles in the annular region of maximum tangential velocity and (b) the nonzero "skirt" of vertical vorticity in this region. The corner portions of the top-hat profile of vertical vorticity become curved; the circulation at the vortex's core radius is not discontinuous. This transition indicates that the turbulent mixing takes place which reduces the cusp in the annular region of tangential velocity maximum. The tangential wind measurements of waterspouts (Leverson et al. 1977), dust devils (Sinclair 1973; Bluestein et al. 2004; Kanak 2005), laboratory-simulated vortices (Church et al. 1979), mobile Doppler radar observations of tornadoes (Bluestein et al. 2007; Tanamachi et al. 2007; Wurman et al. 2007) and tropical cyclones (Mallen et al. 2005) are very good examples of the SRCV.

The purpose of this study is (a) to formulate the SRCV model based on actual tangential wind measurements of dust devils, laboratory- and numerical-simulated vortices, tornadoes, and tropical cyclones, and (b) to show how the SRCV can be transitioned to the RCV. Our analytical SRCV model parameters enable us to evaluate the parameters' distributions and to conduct a critical examination of the tangential velocity, vertical vorticity and circulation profiles' realism. The profiles in the SRCV model are compared with those of the RCV and Burgers (1948)-Rott (1958) vortex.

Corresponding author address: Vincent T. Wood, National Severe Storms Laboratory, 120 David L. Boren, Blvd., Norman, OK 73072. E-mail: Vincent.Wood@noaa.gov

2. WOOD-WHITE VORTEX MODEL

a. Tangential velocity

In order to formulate the SRCV model, we first define a simple analytical vortex model which consists of a tangential velocity (V) increasing from zero at the vortex center ($r = 0$) to a radial distance (R_x), where a maximum tangential velocity (V_x) occurs, and beyond R_x, the velocity decays with increasing radial distance ($r > R_x$). To represent the vortex, we define a non-dimensional radial distance $\rho = r / R_x$ and a tangential-velocity function $\psi(\rho) = V / V_x$ with at least the following properties: $\psi(0) = 0$, $\psi(1) = 1$, $\psi(\infty) = 0$, $\partial\psi / \partial\rho = 0$ at $\rho = 1$ (where ψ has its maximum value), $\partial\psi / \partial\rho > 0$ for $\rho < 1$, $\partial\psi / \partial\rho < 0$ for $\rho > 1$, and $\psi(\rho) > 0$ for $0 < \rho < \infty$. With the properties, the tangential-velocity function may be expressed as

$$\psi(\rho) \equiv \Psi(\rho; q) = \frac{2^{1/q}\rho}{(1+\rho^{2q})^{1/q}}, \quad q > 0, \qquad (1)$$

where the non-dimensional exponent q controls the shape of the tangential-velocity profile. As $q \to \infty$, the profile, for instance, undergoes transition from a smooth, rounded tangential velocity peak to a cusp at $\rho = 1$. The behavior of q on the tangential-velocity function will be discussed in the subsequent sections.

b. Vertical vorticity

Vertical vorticity (ζ) in axisymmetric flow is given by

$$\zeta = \frac{\partial V}{\partial r} + \frac{V}{r}. \qquad (2)$$

Substitution of (1) into (2) yields

$$\zeta_{WWV} = \frac{V_x}{R_x}\left[2\rho^{-1}\Psi - \rho^{(q-1)}\Psi^{(q+1)}\right], \qquad (3)$$

where the subscript in ζ_{WWV} refers to the Wood-White vortex (henceforth WWV) model.

c. Circulation

Circulation is the basic measure of macroscopic rotation in a fluid and is given for an axisymmetric vortex by

$$\Gamma = 2\pi V r \,, \tag{4}$$

where V is tangential velocity component. Substitution of (1) into (4) results in

$$\Gamma_{WWV} = 2\pi V_x R_x \left[\frac{2^{1/q}\rho^2}{(1+\rho^{2q})^{1/q}} \right]. \tag{5}$$

Eqs. (1), (3), and (5) will be used to describe the radial profiles of "evolving" tangential velocity, vertical vorticity, and circulation for the SRCV model as a function of q values in section 5. The inviscid steady-state RCV and the viscous steady-state Burgers (1948)-Rott (1958) vortex models, described in sections 3 and 4, will also be used for purposes of comparison.

3. BURGERS-ROTT VORTEX MODEL

The Burgers (1948)-Rott (1958) vortex (henceforth BRV) is a viscous one-celled vortex model in which fluid spirals in toward the z axis as it rises. The BRV also is a more realistic model than the RCV, because the former model predicts (a) a smooth, rounded maximum at its core radius, owing to the presence of diffusion, and (b) the bell-shaped (or Gaussian-shaped) profile of vertical vorticity.

The normalized tangential velocity distribution of the BRV model, as given by Davies-Jones and Wood (2006), is expressed as

$$V^*_{BRV} \equiv \frac{V_{BRV}}{V_x} = \frac{1.398}{\rho}\left[1-\exp(-K\rho^2)\right],\ \rho \neq 0\,, \tag{6}$$

where $V_x = 0.715 M_\infty / R_x$ is maximum tangential velocity, $M_\infty \equiv \Gamma_\infty / 2\pi$ is angular momentum at infinity, Γ_∞ is circulation at infinity, and $K = 1.2564$. The BRV's core radius is $R_x = (2Kv_e/a)^{1/2}$, where v_e is constant eddy viscosity, and $2a$ is uniform convergence.

The normalized vertical vorticity profile of the BRV, given by

$$\zeta^*_{BRV} \equiv \frac{\zeta_{BRV} R_x}{V_x} = 2.8K\exp(-K\rho^2)\,, \tag{7}$$

predicts that the bell-shaped profile of ζ^*_{BRV} attains its maximum at $\rho = 0$ and approaches zero asymptotically as $\rho \to \infty$.

The normalized circulation of the BRV is obtained as (e.g., Davies-Jones and Wood 2006)

$$\Gamma^*_{BRV} \equiv \frac{\Gamma_{BRV}}{\Gamma_\infty} = 1-\exp(-K\rho^2)\,. \tag{8}$$

4. IDEALIZED RANKINE COMBINED VORTEX

A classic model of inviscid vortex flow is the idealized, steady-state RCV, which consists of an inner core of solid-body rotation (tangential velocity $V_{RCV} \propto r$) and an outer region where $V_{RCV} \propto r^{-1}$. The normalized tangential velocity profile of the RCV is given by

$$V^*_{RCV} = \begin{cases} \rho, & \rho \le 1, \\ \rho^{-1}, & \rho \ge 1. \end{cases} \tag{9}$$

The RCV model produces a normalized vertical vorticity profile which is obtained by substituting (8) into (2), thus yielding

$$\zeta^*_{RCV} = \begin{cases} 2, & \rho \le 1, \\ 0, & \rho \ge 1. \end{cases} \tag{10}$$

The model in (10) predicts a top-hat profile of ζ^*_{RCV} in the vortex embedded in an irrotational (potential vortex) environment. The model, however, suffers from the fact that ζ^*_{RCV} has the discontinuous jump from constant to zero in the annular region of maximum tangential velocity.

The normalized circulation ($\Gamma^*_{RCV} = \Gamma_{RCV}/\Gamma_\infty$) of the RCV is given by

$$\Gamma^*_{RCV} \begin{cases} = \rho^2, & \rho \le 1, \\ = 1, & \rho \ge 1. \end{cases} \tag{11}$$

The behavior of the circulation will be described in section 5.

5. SKIRTED RANKINE COMBINED VORTEX

To facilitate comparison with radial profiles of tangential wind, vertical vorticity and circulation, normalized composites are constructed that beneficially preserve the underlying tangential wind, vertical vorticity and circulation structures. Each individual profile is expressed in non-dimensional form utilizing the typical scales, V_x and R_x. The normalized tangential velocity and vertical vorticity profile of the SRCV model, respectively, are given by $V^*_{SRCV} \equiv V_{WWV}/V_x$ and $\zeta^*_{SRCV} \equiv \zeta_{WWV} R_x / V_x$. The normalized circulation of the SRCV model is obtained by normalizing (5) by $2\pi V_x R_x$, thus resulting in $\Gamma^*_{SRCV} \equiv \Gamma_{WWV}/(2\pi V_x R_x)$.

Figure 1 presents the radial variations of V^*_{SRCV} as a function of q values with increasing ρ. Clearly, $\Psi(0;q) = 0$; $\Psi(1;q) = 1$; and $\Psi(\infty;q) = 0$. Taking the limit of (1) as $q \to \infty$, $\Psi(\rho;\infty) \to \rho$ for $\rho \le 1$ which means that V^*_{SRCV} approaches the inner core of

solid-body rotation. This agrees with (9). Furthermore, $\Psi(\rho;\infty) \to \rho^{-1}$ for $\rho \geq 1$, indicative of the fact that V^*_{SRCV} decreases and tends asymptotically to the value given by a potential flow in which $V^*_{SRCV} \propto \rho^{-1}$. This favorably agrees with (9).

In the annular region of the normalized tangential velocity peak, the tangential velocity profile shape at low q values is broader than the sharply peaked profile of the RCV (Fig. 1). Increasing q to very large values changes the broader tangential velocity profile to a cusp in the velocity profile at $\rho = 1$.

The SRCV compares favorably with various observations, namely, Sinclair (1973) in his observational studies of dust devils (his Figs. 11 and 12), Church et al. (1979) in their laboratory simulation studies of tornado-like vortices (their Figs. 14 and 17), Bluestein et al. (2004) in their mobile Doppler radar observations of dust devils (their Fig. 9), Kanak (2005) in her numerical simulation of dust devil-scale vortices (her Figs. 7 and 8), Bluestein et al. (2007) and Tanamachi et al. (2007) in their mobile Doppler radar observations of tornadoes, and Mallen et al. (2005) in their aircraft observational studies of tropical cyclones. In a real flow, the cusp in the tangential velocity profile would have been rounded off and reduced by diffusion.

The roles of q on behaving the ζ^*_{SRCV} profiles in the SRCV model are presented in Fig. 2. It is worthy noting in the figure that ζ^*_{BRV} at $\rho = 0$ in (7) is higher than ζ^*_{RCV}, owing to the $2.8K$ term. As predicted by (3), the radial profiles of ζ^*_{SRCV} of the SRCV are bell-shaped at low values of q. Taking the limit of (3) as $q \to \infty$, the bell-shaped profile of ζ^*_{SRCV} evolves to a top-hat configuration which agrees well with (10). The SRCV is characterized by the relatively slow tangential velocity decay in conjunction with a skirt of non-zero vertical vorticity just outside $\rho = 1$ in the sense that the peripheral circulation may be small compared to that of the vortex core. In addition, it is worthy noting that at $\rho = 1$, ζ^*_{SRCV} reduces to one half of the constant value of $\zeta^*_{RCV} = 2$, regardless of the q values. At low values of q, the slow underlying monotonic decrease of ζ^*_{SRCV} ensures appreciable vertical vorticity out to large ρ. This is in striking contrast to the characteristic zero vertical vorticity of the RCV at and beyond $\rho = 1$. In tropical cyclone studies of Mallen et al. (2005), their computed relative vorticity values, when normalized, have been shown to be 1.0 at $\rho = 1$, which favorably agrees with Fig. 2.

At $\rho = 0$, (3) is reduced to

$$\zeta^*_{SRCV} = 2^{1+1/q}, \quad q > 0. \qquad (12)$$

(12) reveals that as $q \to \infty$, ζ^*_{SRCV} asymptotes to 2, which is a constant value for ζ^*_{RCV}, favorably comparing with (10). Furthermore, $\zeta^*_{SRCV} \to \infty$ as $q \to 0$ (Fig. 3).

Figure 4 presents the radial variations of Γ^*_{SRCV} with varying values of q. According to Davies-Jones and Wood (2006), circulations around material horizontal circles in the RCV are conserved. Inside the RCV core, Γ^*_{RCV} varies as ρ^2, as shown in (11). From the core wall of the RCV to radial infinity, Γ^*_{RCV} is constant because the outer flow is irrotational. This is not the case for the SRCV and BRV, except for very large q values in the SRCV. It is interesting to note in Fig. 4 that $\Gamma^*_{SRCV} \to \rho^2$ as $q \to \infty$ at $\rho < 1$, which agrees with (11). At $\rho = 1$, $\Gamma^*_{SRCV} = 1$, regardless of the q values. Furthermore, at $\rho > 1$, $\Gamma^*_{SRCV} \to 1$ as $q \to \infty$, which also agrees with (11). The normalized circulations of the SRCV favorably agree with computed circulations based on mobile Doppler radar observations of tornadoes (Bluestein et al. 2007; Tanamachi et al. 2007).

6. CONCLUSIONS

The "skirted" Rankine combined vortex model, which is derived from the Wood-White vortex model, has been formulated based on prior studies of actual tangential wind measurements of dust devils, laboratory- and numerical-simulated tornado-like vortices, tornadoes, waterspouts, and tropical cyclones. The SRCV is a version of the RCV in which a smooth transition is created between the inner and outer profiles in the annular region of maximum tangential velocity.

The RCV is used as the basis for a number of simple descriptions of atmospheric vortices. In light of observations, laboratory experiments and numerical simulations of atmospheric vortices, the unrealistic RCV lacks the girth in the tangential wind, vertical vorticity, and circulation structures, owing to the simplicity of the RCV model. This is in sharp contrast to the SRCV whose a smooth, rounded tangential velocity peak does not result in the inherent discontinuity of vertical vorticity and circulation at its core radius, owing to the sophistication of the SRCV model. The model favorably compares with the observed profiles of tangential wind, vertical vorticity and circulation.

The SRCV model has several potential applications. Maximum vortex wind speeds, their radii, and q values may be deduced by least squares fitting of the SRCV model to those measured with a high-resolution, mobile Doppler radar. The second application may be related to simulated single-Doppler velocity signatures of mesocyclones and tornadoes (e.g., Wood and Brown 2002, Brown et al. 2002). The

third application is numerical/analytical model initialization in which initial conditions of tangential velocity can be defined (e.g., Dowell et al. 2005).

7. ACKNOWLEDGMENTS

The authors thank Bob Davies-Jones of NSSL and John Snow of National Weather Center for reading and making input and suggestions in this paper.

8. REFERENCES

Bluestein, H. B., C. C. Weiss, and A. L. Pazmany, 2004: Doppler radar observations of dust devils in Texas. *Mon. Wea. Rev.,* **132,** 209-224.

_____, C. C. Weiss, M. M. French, E. M Holthaus, R. L. Tanamachi, S. Frashier, and A. L. Pazmany, 2007: The structure of tornadoes near Attica, Kansas, on 12 May 2004: High-resolution, mobile, Doppler radar observations. *Mon. Wea. Rev.,* **135,** 475-506.

Brown, R. A., and V. T. Wood, 2002: Improved tornado detection using simulated and actual WSR-88D data with enhanced resolution. *J. Atmos. Oceanic Technol.,* **19,** 1759-1771.

Burgers, J. M., 1948: A mathematical model illustrating the theory of turbulence. *Adv. Appl. Mech.,* **1,** 197-199.

Church, C. R., J. T. Snow, G. L. Baker, and E. M. Agee, 1979: Characteristics of tornado-like vortices as a function of swirl ratio: a laboratory investigation. *J. Atmos. Sci.,* **36,** 1755-1776.

Davies-Jones, R. P., and V. T. Wood, 2006: Simulated Doppler velocity signatures of evolving tornado-like vortices. *J. Atmos. Oceanic Technol.,* **23,** 1029-1048.

Dowell, D. C., C. R. Alexander, J. M. Wurman, and L. J. Wicker, 2005: Centrifuging of hydrometeors and debris in tornadoes: radar-reflectivity patterns and wind-measurement errors. *Mon. Wea. Rev.,* **133,** 1501-1524.

Kanak, K. M., 2005; Numerical simulation of dust devil-scale vortices. *Q. J. R. Meteorol. Soc.,* **131,** 1271-1292.

Leverson, V. H., P. C. Sinclair, and J. H. Golden, 1977: Waterspout wind, temperature and pressure structure deduced from aircraft measurements. *Mon. Wea. Rev.,* **105,** 715-733.

Mallen, K. J., M. T. Montgomery, and B. Wang, 2005: Reexamining the near-core radial structure of the tropical cyclone primary circulation: Implications for vortex resiliency. *J. Atmos. Sci.,* **62,** 408-425.

Rankine, W. J. M., 1882: *A Manual of Applied Physics.* 10th ed. Charles Griff and Company, London, 663 pp.

Rott, N., 1958: On the viscous core of a line vortex. *Z. Angew. Math. Physik,* **96,** 543-553.

Sinclair, P. C., 1973: The lower structure of dust devils. *J. Atmos. Sci.,* **30,** 1599-1619.

Tanamachi, R. L., H. B. Bluestein, W.-C. Lee, M. Bell, and A. Pazmany, 2007: Ground-based velocity track display (GBVTD) analysis of W-band Doppler radar data in a tornado near Stockton, Kansas, on 15 May 1999. *Mon. Wea. Rev,* **135,** 783-800.

Wood, V. T., and R. A. Brown, 1997: Effects of radar sampling on single-Doppler velocity signatures of mesocyclones and tornadoes. *Wea. Forecasting,* **12,** 928-938.

Wurman, J., C. Alexander, P. Robinson, and Y. Richardson, 2007: Low-level winds in tornadoes and potential catastrophic tornado impacts in urban areas. *Bull. Amer. Soc.,* **88,** 31-46.

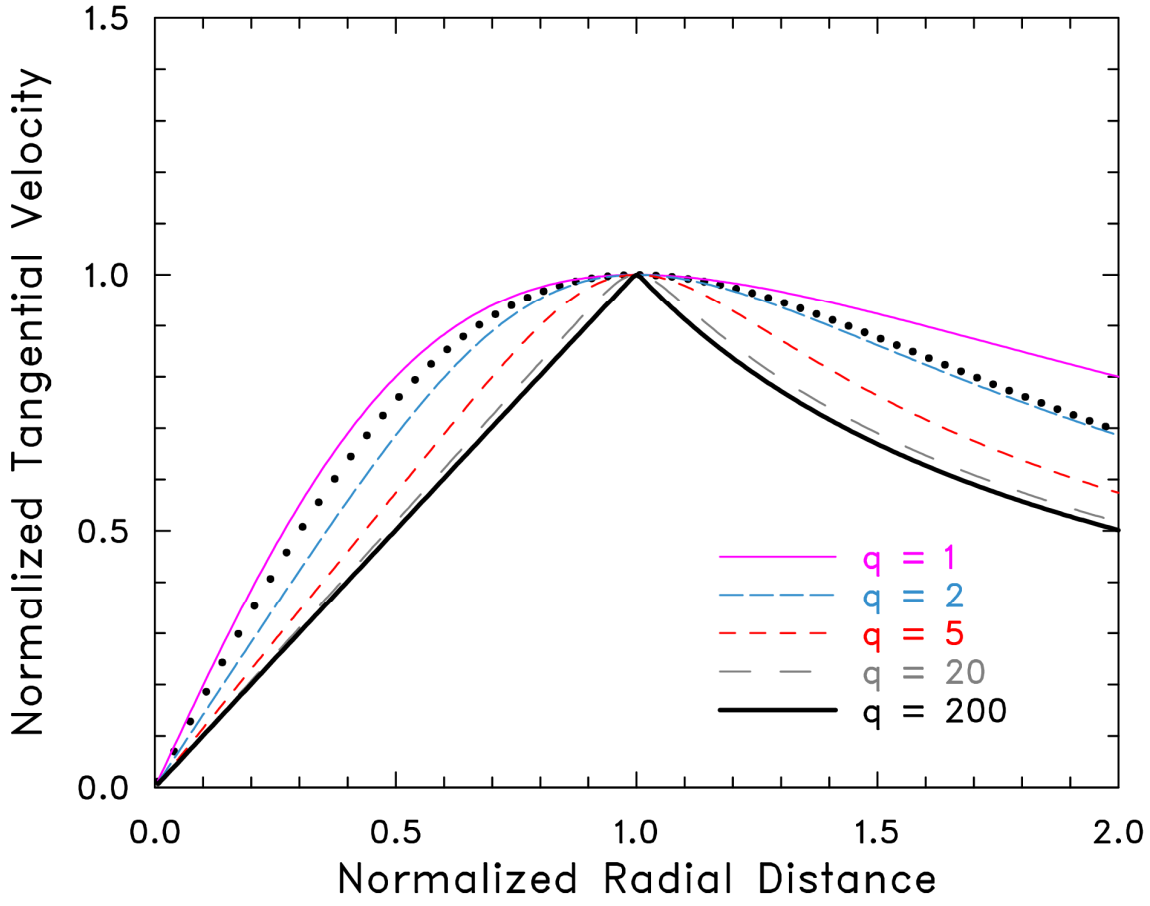

Fig. 1. Radial profiles of normalized tangential velocity ($V^* = V / V_x$) as a function of q values. Solid (dotted) black curve represents the idealized Rankine combined (Burgers-Rott) vortex for purpose of comparison. The normalized radial distance is $\rho = r / R_x$.

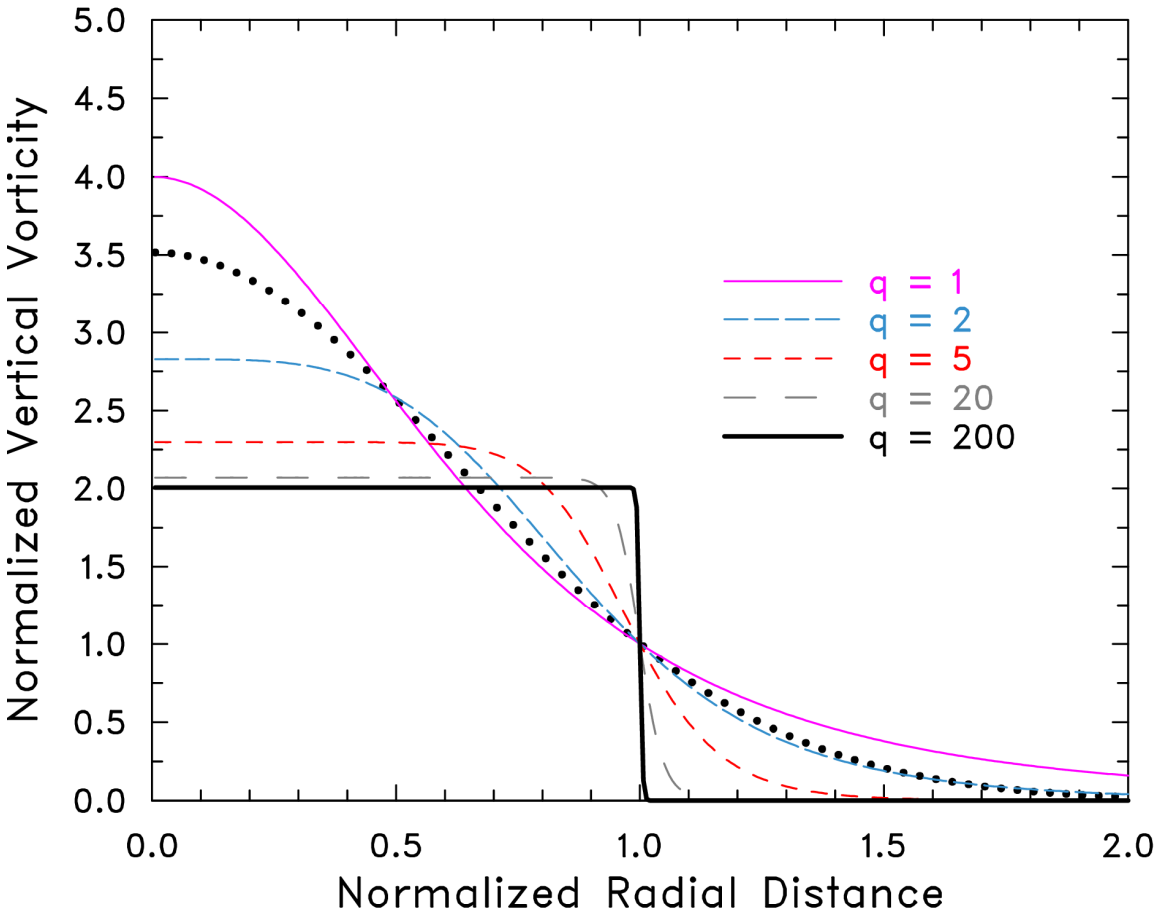

Fig. 2. Radial profiles of normalized vertical vorticity ($\zeta^* = \zeta R_x / V_x$) as a function of q values. Solid (dotted) black curve represents the idealized Rankine combined (Burgers-Rott) vortex for purpose of comparison. The normalized radial distance is $\rho = r / R_x$.

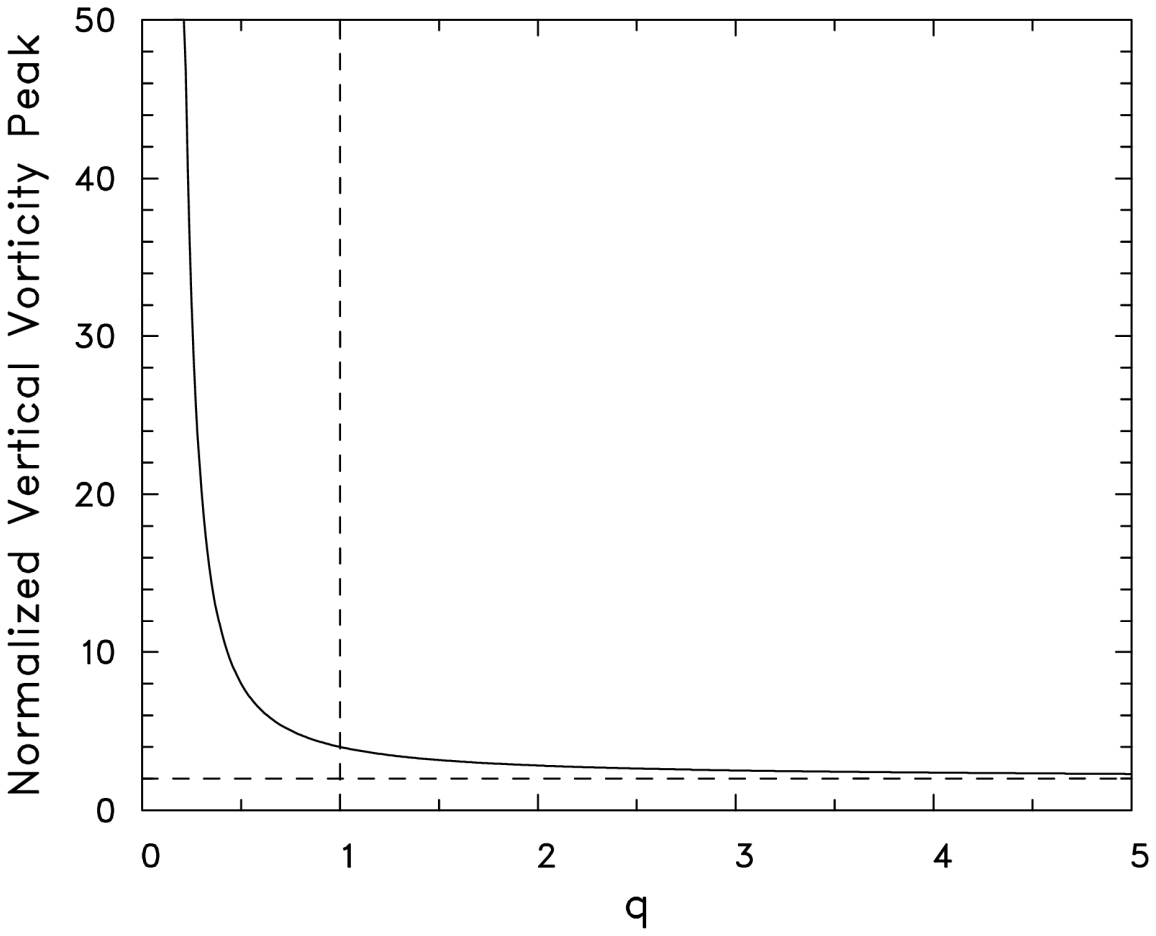

Fig. 3. Normalized vertical vorticity peak as a function of q values at the axis of the vortex ($\rho = 0$).

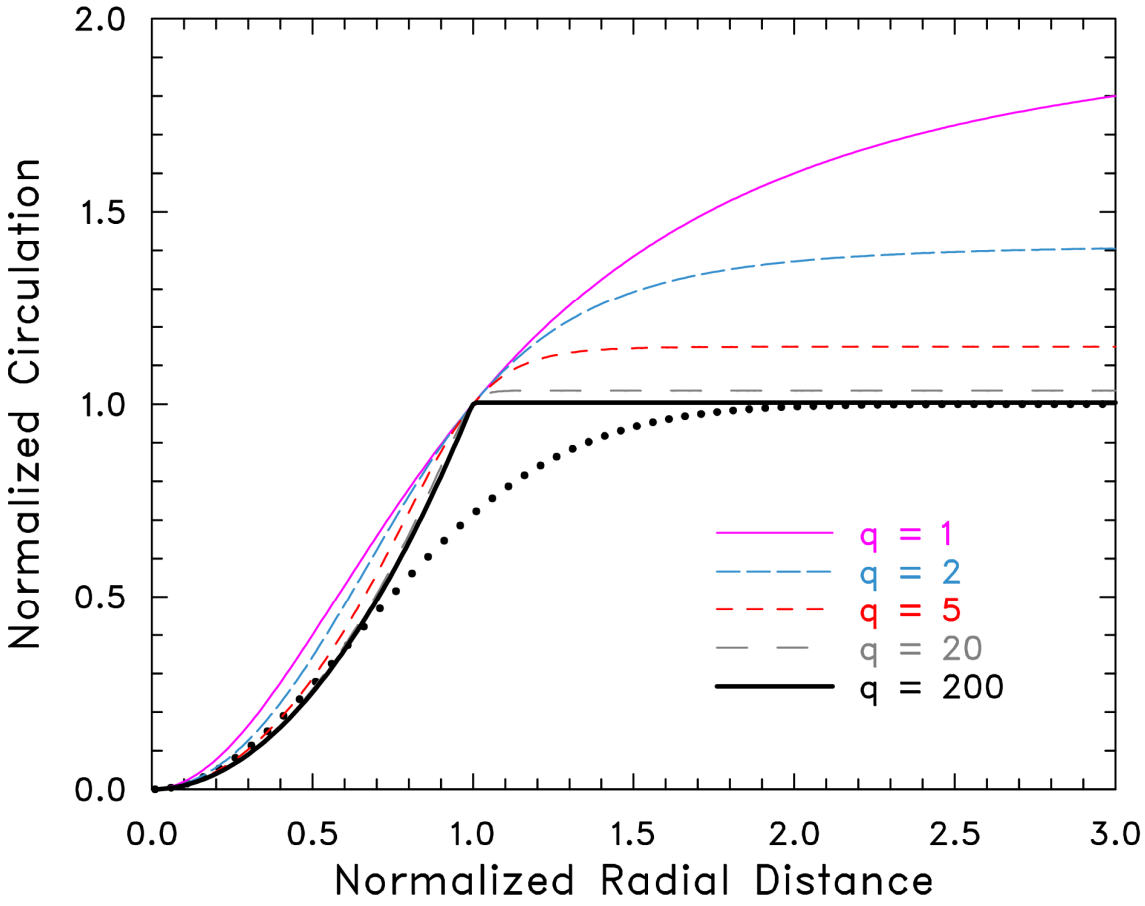

Fig. 4. Radial profiles of normalized circulation ($\Gamma^* = \Gamma / \Gamma_\infty$) as a function of q values. Solid (dotted) black curve represents the idealized Rankine combined (Burgers-Rott) vortex for purpose of comparison. The normalized radial distance is $\rho = r / R_x$.